ИНЖЕНЕРИЯ ЖӘНЕ ИНЖЕНЕРЛІК ІС
ИНЖЕНЕРИЯ И ИНЖЕНЕРНОЕ ДЕЛО
ENGINEERING AND ENGINEERING

МЕТАЛЛУРГИЯ
МЕТАЛЛУРГИЯ
METALLURGY

DOI 10.51885/1561-4212_2025_1_5
IRSTI 53.49.21

**I.K. Abizhanova[1], D.B. Buitkenov[2], N.M. Magazov[1], A.E. Kusainov[1], S.A. Abdulina[1]**
[1]D. Serikbaev East Kazakhstan Technical University, Ust-Kamenogorsk, Kazakhstan
*E-mail: www.indiko@mail.ru**
*E-mail: magazovn@gmail.com*
*E-mail: arys20055@gmail.com*
*E-mail: abdulina.saule@mail.ru*
[2]S. Amanzholov East Kazakhstan University, Ust-Kamenogorsk, Kazakhstan
*E-mail: buitkenovd@mail.ru*

# INVESTIGATION OF THE EFFECT OF THE SPRAYING DISTANCE ON THE PROPERTIES OF $CR_3C_2$-NICR METAL-CERAMIC COATINGS OBTAINED BY THE HVOF METHOD

# HVOF ӘДІСІМЕН АЛЫНҒАН $CR_3C_2$-NICR МЕТАЛЛ КЕРАМИКАЛЫҚ ЖАБЫНДАРЫНЫҢ ҚАСИЕТТЕРІНЕ БҮРКУ ҚАШЫҚТЫҒЫНЫҢ ӘСЕРІН ЗЕРТТЕУ

# ИССЛЕДОВАНИЕ ВЛИЯНИЯ ДИСТАНЦИИ НАПЫЛЕНИЯ НА СВОЙСТВА МЕТАЛЛОКЕРАМИЧЕСКИХ ПОКРЫТИЙ $CR_3C_2$-NICR, ПОЛУЧЕННЫХ МЕТОДОМ HVOF

***Abstract.*** *In this paper, $Cr_3C_2$-NiCr metal-ceramic coatings obtained by high-velocity oxygen fuel spraying (HVOF) at various spraying distances are studied. A detailed morphological characterization of the cross section of the coatings was carried out using scanning electron microscopy (SEM) with backscattered electrons (BSE). It was found that the particle size of chromium carbide $Cr_3C_2$ varies depending on the deposition distance. Morphology analysis also revealed the distribution of pores, which is important for the wear resistance of coatings. It was also discovered that as the spraying distance increases, the surface roughness of the coatings also increases. Hardness tests indicated that the coating hardness is influenced by the level of decarburization and can be associated with the kinetic energy of the particles and the density of dislocations in the coating. Furthermore, the impact of spraying distance on the friction coefficient of the coatings was examined, which is essential for optimizing their performance in wear conditions.These results can be useful in the development and optimization of cermet coatings to increase their wear resistance and efficiency in various industrial conditions.*
***Keywords****: HVOF; cermet coatings; $Cr_3C_2$-NiCr; microstructure; hardness; SEM analysis; coefficient of friction; surface roughness.*

***Аңдатпа.*** *Бұл мақалада әртүрлі бүрку қашықтықтарында жоғары жылдамдықты оттегі-отынды бүрку (HVOF) әдісімен алынған $Cr_3C_2$-NiCr металл керамикалық жабындары зерттелген. Кері шашыраңқы электрондары (BSE) бар сканерлеуші электронды микроскопияны (SEM) пайдалана отырып, жабындардың көлденең қимасының егжей-тегжейлі морфологиялық сипаттамасы жасалды. $Cr_3C_2$ бөлшектерінің мөлшері бүрку қашықтығына байланысты өзгеретіні анықталды. Морфологияны талдау жабындардың тозуға төзімділігіне әсер ететін кеуектердің таралуын анықтады. Сондай-ақ, бүрку қашықтығы ұлғайған сайын жабын бетінің кедір-бұдырлығы ұлғаятындығы анықталды. Жабындардың қаттылығын өлшеу жабындардың қаттылығы декарбонизация дәрежесіне байланысты екенін және бөлшектердің кинетикалық энергиясына*

*және жабындағы дислокация мөлшеріне байланысты болуы мүмкін екенін көрсетті. Сонымен қатар, тозу жағдайында қолдануды оңтайландыру үшін маңызды бүрку қашықтығының жабындардың үйкеліс коэффициентіне әсері зерттелді. Бұл нәтижелер әртүрлі өнеркәсіптік жағдайларда олардың тозуға төзімділігі мен тиімділігін арттыру үшін металл керамикалық жабындарды жобалау және оңтайландыру кезінде пайдалы болуы мүмкін.*

***Түйін сөздер**: жоғары жылдамдықты оттегі-отынды бүрку; металл керамикалық жабын; $Cr_3C_2$-NiCr; микроқұрылым; қаттылық; СЭМ талдау; үйкеліс коэффициенті; беттің кедір-бұдырлығы.*

***Аннотация**. В данной статье исследованы металлокерамические покрытия $Cr_3C_2$-NiCr, полученные методом высокоскоростного кислородно-топливного напыления (HVOF) при различных дистанциях напыления. С использованием сканирующей электронной микроскопии (SEM) с обратно рассеянными электронами (BSE) была проведена детальная морфологическая характеристика поперечного сечения покрытий. Установлено, что размер частиц карбида хрома $Cr_3C_2$ варьируется в зависимости от расстояния напыления. Анализ морфологии также позволил выявить распределение пор, что имеет значение для износостойкости покрытий. Также было обнаружено, что с увеличением расстояния напыления увеличивается шероховатость поверхности покрытий. Измерение твердости покрытий показало, что она зависит от степени обезуглероживания и может быть связана с кинетической энергией частиц и количеством дислокаций в покрытии. Кроме того, исследовано влияние расстояния напыления на коэффициент трения покрытий, что важно для оптимизации их применения в условиях износа. Эти результаты могут быть полезны при разработке и оптимизации металлокерамических покрытий для повышения их износостойкости и эффективности в различных промышленных условиях.*

***Ключевые слова:** высокоскоростное кислородно-топливное напыление; металло-керамические покрытия; $Cr_3C_2$-NiCr; микроструктура; твердость; СЭМ анализ; коэффициент трения; шероховатость поверхности.*

*Introduction.* In the world, 90% of steel is produced by using continuous casting machines. The liquid steel directed into the continuous casting machine is poured from the ladle into the intermediate ladle, and then from the intermediate ladle into the mold, as a result of which the steel crystallizes with a certain thickness of the shell taking the form of a mold (Liu, Zhu and Li, 2019a).

The crystallizer must withstand all-round mechanical and thermal loads (Moro et al., 2017; Ryu et al., 2023). For this reason, very high demands are placed on the strength, thermal conductivity, wear resistance and resistance to high-temperature corrosion of the mold surface.

The material (copper) of the copper crystallizer has low mechanical strength and quickly fails. Extremely high temperature on the hot surface in the meniscus area causes swelling of the form (Velicka et al., 2009; Moro et al., 2019). Instability of the meniscus flow can lead to uneven heat transfer, in addition to trapping mold flux in the solidifying shell (Swain et al., 2023). Therefore, in order to avoid very dangerous damage that can lead to failure of the continuous caster, it is necessary to strengthen the surface of the mold.

The most promising direction to reduce the intensity of wear of the working walls of the mold is currently the application of protective coatings (Novak et al., 2018). The coating process on the surface of the mold mainly includes electroplating, thermal spraying and laser surfacing (Liu, Zhu and Li, 2019a).

However, the electroplating and laser cladding method has a number of disadvantages. Such as high power consumption, waste plating fluid contamination and high cooling rate, which may lead to internal cracking of the coating (Berger, 2015; Bolelli, L.-M. Berger, et al., 2016).

In this regard, new technologies for surface treatment are being actively developed. Among them, thermal spraying technology is an effective method for applying heat-resistant and resistant materials to the surface of metallurgical equipment. Different thermal spraying methods are used to apply protective coatings, such as plasma spraying, arc spraying, cold spray coating and high-velocity oxygen fuel (HVOF) (J.G. La Barbera-Sosa et al., 2010). HVOF coating has more

advantages compared to other thermal spraying technologies, because it is possible to achieve lower porosity, good adhesive strength, high hardness and density (Akhtari Zavareh et al., 2015). The method allows you to control the thickness of the coating and apply a wear-resistant coating only to the lower, most worn part of the mold.

The main most suitable materials for spraying with HVOF technology are WC-Co (Guilemany et al., 1997; Akhtari Zavareh et al., 2015) and NiCr-$Cr_3C_2$ (Zhu, Wang and Lu, 2019; Govande et al., 2022). However, $Cr_3C_2$-25NiCr coatings are more suitable for crystallizer operating conditions and can be used at temperatures below 930°C (Liu, Zhu and Li, 2019b; Yang et al., 2022). $Cr_3C_2$-NiCr provides sufficient resistance to oxidation at intense and consistently high temperatures with taking into account the $Cr_2O_3$ layer (Alroy, Kamaraj and Sivakumar, 2023).

In (Du et al., 2019; Ham et al., 2021; Zhang et al., 2021; Rubino et al., 2023), the coating qualities of $Cr_3C_2$-NiCr powder obtained by different technologies were studied. Compared to other thermal spraying technologies, high-speed oxygen-fuel spraying has proven to be a simple and effective way to improve wear resistance. However, the production of high-quality coatings depends not only on the technology employed but also on the HVOF spray system and the parameters used during spraying. The authors (Zimmermann and Kreye, 1996) conducted experiments with high-speed oxygen-fuel (HVOF) with Diamond Jet (DJ) 2600 and 2700, P-5000, Jet Kote and Top Gun with changes in particle velocity to study their effect on the microstructure and properties of $Cr_3C_2$-NiCr coatings. The results show that $Cr_3C_2$-NiCr coatings of high density, high adhesion strength and high wear resistance can be obtained with all HVOF systems used. However, the microstructure and properties of the coatings are primarily influenced by the extent of oxidation and carbon loss in the material during the spraying process (Matikainen, Koivuluoto and Vuoristo, 2020; Mahade et al., 2021; Shi et al., 2022; Ozkan, 2023). The author of the literature (Maheshwaran et al., 2022) also identified that the flow rate is the most influential factor in these processes of sprayed HVOF, followed by the powder feed rate, spray distance and oxygen flow rate.

Autors 0 compared the particle flight properties and coating characteristics of powders under different process parameters. They found that for $Cr_3C_2$-NiCr powder, the particle velocity increased with lower fuel consumption and shorter spray distance. As the particle velocity increased, the deposition efficiency decreased. Shorter particle residence time in the hot stream resulted in a lower melting rate and a higher probability of particle rebound at high velocities.

Based on this, the importance of the correct selection of the spraying parameter is determined. The process parameters are independent variables, and their result consists of dependent variables, including thickness, porosity, hardness, toughness, wear, corrosion, and oxidation resistance.

Currently, the actual proportion of applying thermally sprayed coatings to continuous casting crystallizers does not exceed 5% (Guilemany et al., 1997). Thus, the promotion and application of thermal coatings on production sites mainly depends on the improvement of auxiliary coating equipment and precise control of the parameters of the coating process.

This article focuses on the optimization of the coating process, aimed at improving the surface properties of molds. HVOF coatings require the selection of optimal spray modes. HVOF Termika-3 equipment, located in the scientific and production company “PlasmaScience” LLP (Ust-Kamenogorsk, Kazakhstan), will be used to carry out experimental work.

*Materials and methods of research.* In the present study, $Cr_3C_2$-NiCr powder (75/25) with particle size ranging from 20 to 32 μm was used to coat copper samples. Before coating, the substrate surfaces were polished with MIRKA sandpaper to a grain size of 2500 to achieve a uniform and even surface. Then they were sandblasted for better adhesion of the sprayed coating.

The HVOF TERMIKA-3 installation (Plasmacenter, St.Petersburg, Russia) was used as the spraying equipment. Three coatings with varying spraying distances were obtained: $L_1$ – 200 mm, $L_2$ – 250 mm, $L_3$ – 300 mm.

To identify the phase composition of the coating, X-ray diffraction analysis (XRD) was performed. An X'PertPro X-ray diffractometer (Philips Corporation, Eindhoven, the Netherlands) with a Cu-Kα anode (λ = 0.154 nm) was used for this purpose. The following parameters were used: tube voltage U = 40 kV, tube current I = 30 mA. Analysis and processing were performed using OriginPro software. Data were collected in the 2θ range from 20° to 90° with a step of 0.02° and a counting time of 1 second per step.

The coatings microstructural features were characterized using scanning electron microscopy (TESCAN VEGA 3 LMH, Czech Republic) with magnifications of 1650x and 5000x. The metallographic microscope Altami MET 5C (OOO Altami, St. Petersburg, Russia) was used to evaluate porosity.

The surface roughness ($R_a$) of the coatings was measured for each sample in five measurements using a model 130 profilometer (PROTON, Moscow, Russia).

Using a FISCHERSCOPE HM2000 S (Helmut Fischer GmbH, Germany), the mechanical properties of the samples were measured at a load of 2000 mN and an exposure time of 20 seconds.

Tribological friction tests were carried out on a TRB3 tribometer using the standard ball-on-disk method. The counterbody was made of 100Cr6 coated steel, with a load of 6 N and a friction path of 100 m.

Results and discussion. Figure 1 shows a $Cr_3C_2$-NiCr powder with an almost spherical morphology consisting of a subset of agglomerate particles. An analysis of the literature confirms the presence of Ni in the light gray zone as an agglomerating phase in irregularly shaped areas connecting chromium carbide particles that look like dark gray zones.

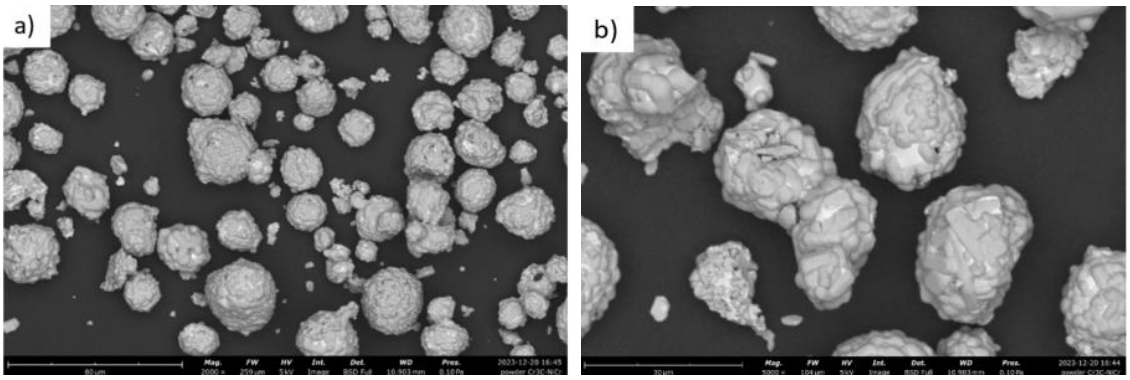


**Figure 1.** Morphology of $Cr_3C_2$-NiCr powder: a) 1650x; b)5000x;
*Note – compiled by the author*s

Figure 2 shows the X-ray images of the original $Cr_3C_2$-25NiCr powder and $L_1$, $L_2$ and $L_3$ coatings. Two main phases can be detected in the initial powder: (1) binding $CrNi_3$, which provides high adhesion strength as well as fracture toughness, and (2) solid $Cr_3C_2$, which provides higher hardness and wear resistance. The carbide phases $Cr_7C_3$, $Cr_{23}C_6$ were found in the coating formed during decarburization of $Cr_3C_2$. Similar phases have been found in other works (He and Lavernia, 2001; Hou et al., 2004; Akhtari Zavareh et al., 2015; Bolelli, L. M. Berger, et al., 2016a; Wang et al., 2016; Ke et al., 2017; Matikainen, Koivuluoto and Vuoristo, 2020; Ham et al., 2021).

Decarburization of $Cr_3C_2$ indicated the influence of deposition parameters on the phase structure of the coating. The $L_1$ coating contains more of the $Cr_3C_2$ phase, which means relatively little decarburization of $Cr_3C_2$ to $Cr_7C_3$. The high percentage of preserved $Cr_3C_2$ grains was obvious. The crystal peaks of this phase were clearly expressed on the diffractogram. Given the temperature regime, HVOF can melt NiCr and a small amount of $Cr_3C_2$, and a new phase is

formed less.

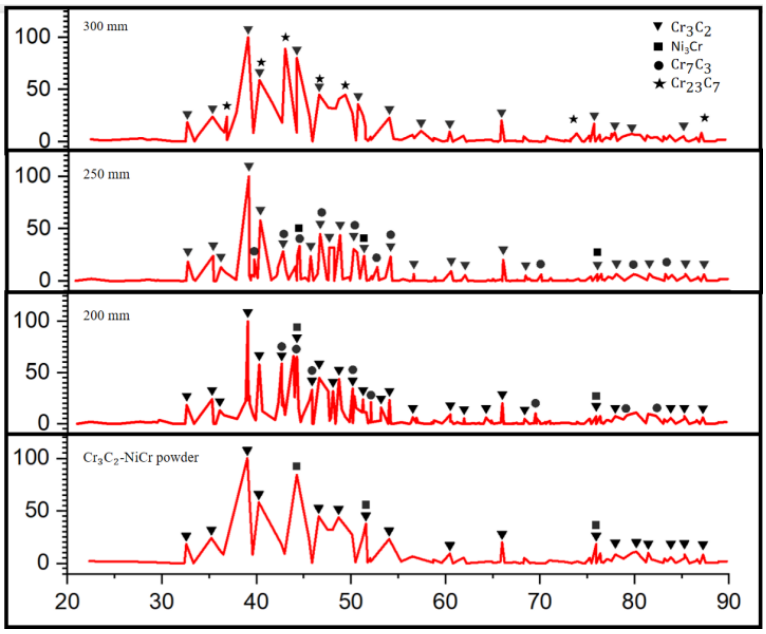


**Figure 2.** X-ray images of the initial $Cr_3C_2$-NiCr powder and coatings with spray distances $L_1$= 200 mm, $L_2$=250 mm and $L_3$=300 mm

*Note – compiled by the authors*

It is noticeable that with a decrease in the spray distance, the intensity of the peaks of chromium carbide $Cr_3C_2$ increases (Figure 2). Moreover, the NiCr binding phase was not detected in the $L_3$ sample. Instead of this phase, $Cr_{23}C_6$ was formed due to decarbonization of the carbide phase. Mohanty et al. (Muthu et al., 2020) also noted a phase change from $Cr_3C_2$ to $Cr_{23}C_6$ during sputtering. This can be explained by long exposure to flame (Muthu et al., 2020). Another reason may be the high speed of the particle spraying process.

However, according to Zimmerman and Kreye (Zimmermann and Kreye, 1996), the presence of in the deposited coating cannot be confirmed solely by X-ray diffraction, since the main diffraction peaks of $Cr_7C_3$ and $Cr_{23}C_6$ coincide with the lines associated with NiCr and $Cr_3C_2$. In addition, the decarburization of $Cr_3C_2$ is apparently associated with the heating of $Cr_3C_2$ spray particles. As confirmed by the results of previous studies, the main cause of carbon loss and changes in the content of carbides is the rebound of $Cr_3C_2$ particles during coating formation (Sahraoui, N. E. Fenineche, et al., 2003). It should also be remembered that X-rays penetrate only about 5 microns of the coating.

Figure 3 shows the morphology of the cross – section of coatings obtained at different spraying distances: $L_1$ – 200 mm; $L_2$ – 250 mm; $L_3$ – 300 mm. The morphology of the cross-section of all coatings was analyzed using SEM using backscattered electron imaging (BSE). For convenience, the analysis was carried out at various magnifications to obtain more detailed information about the structure of the coating and assess its characteristics.

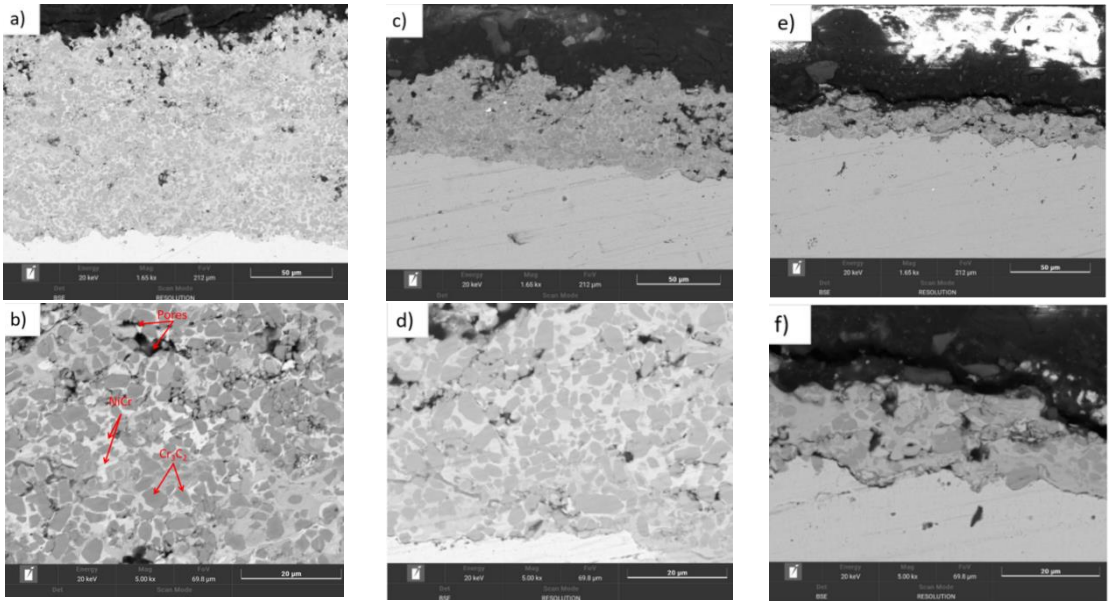


**Figure 3.** SEM images of the morphology of the cross-section of $Cr_3C_2$-NiCr coatings obtained by changing the deposition distance. (a,b) 200 mm; (c,d) 250 mm; (e,f) 300 mm
*Note – compiled by the authors*

According to (Bolelli, L. M. Berger, et al., 2016b; Rovatti et al., 2017; Ke et al., 2019; Ozkan, 2023; Rubino et al., 2023), dark gray contrast particles are relatively evenly distributed throughout the coating; it is assumed that this is the $Cr_3C_2$ phase. The lighter gray matrix is presumably a matrix with a high nickel content. The phase of the cermet coating was NiCr with embedded Cr-based carbide. The reason is that the sprayed powder for the cermet coating was formed from small particles of NiCr-$Cr_3C_2$ agglomerate mixed with NiCr alloy powder, and the melting point of $Cr_3C_2$ is higher than that of NiCr. The high-magnification image in Figure 3b shows that the size of dark gray contrast particles ranges from about 4.3 microns for $L_1$, 4.4 microns for $L_2$ and 3.8 microns for $L_3$. There is evidence of a small amount of small-scale porosity (small black elements), with an average value of 4.3%±0.5. The same microstructure is observed in other coatings of different thicknesses.

Additionally, evenly distributed pores with smaller sizes are generally preferred, as coatings with larger pores tend to have localized and more pronounced areas of wear-related damage (Sahraoui, N.-E. Fenineche, et al., 2003). The proportion of carbide and porosity revealed in the cross-section images are within the range usually observed for coatings of this type sprayed with HVOF. $L_1$ coatings fit snugly to the base, without cracks and failures, there are no signs of peeling. In $L_1$, porosity increases closer to the surface. The carbide phase has an irregular shape and is not plastically deformed, while the metal bundle is plastically deformed. $L_2$ it is also seen that the carbide phase has an irregular shape and is not plastically deformed, while the metal bundle is plastically deformed. The carbide phase is well dissolved. However, there is a slight detachment from the substrate in the $L_2$ coating. $L_3$ carbide particles were plastically deformed due to the corresponding long stay in the hot jet. Microcracks and separation of the interface with the substrate indicate the concentration of stress in the coating (Ham et al., 2021). The coating thickness on the cross-section of the samples ranged from 25.6 μm to 120.91 μm. As the spraying distance increased, the thickness of the metal-ceramic coating decreased.

The average surface roughness of the coatings $L_1$, $L_2$ and $L_3$ is equal to $R_a$ = 0.672 microns; $R_a$ = 0.743 microns; $R_a$ = 0.808 microns, respectively. The primary parameter used to assess

roughness was the $R_a$ value, which represents the arithmetic mean deviation of the surface profile. It was found that the surface roughness varies depending on the spraying distance. To evaluate the roughness, the Ra value was used, which is the permissible arithmetic deviation of the surface. The values of the roughness of the coatings are shown in Figure 4.

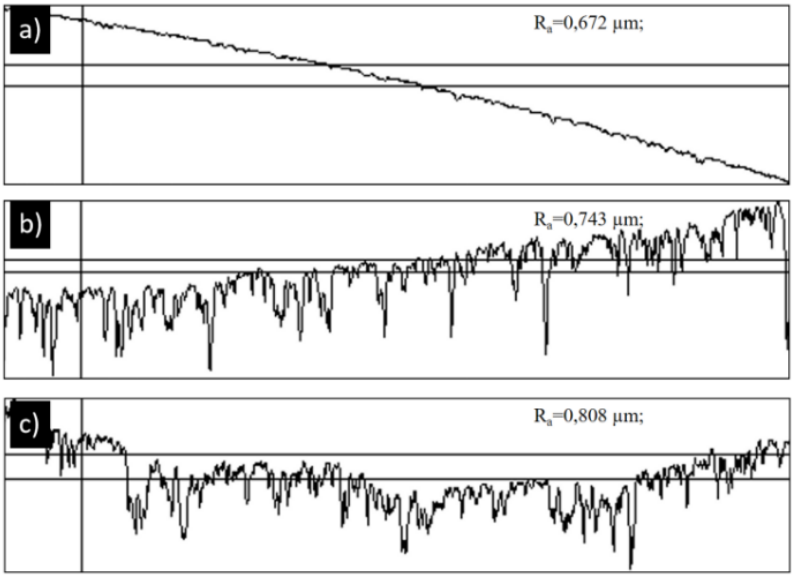


**Figure 4.** Surface roughness of the $Cr_3C_2$-NiCr coating: a) 200 mm;b) 250 mm; c) 300 mm;
*Note – compiled by the authors*

The $Cr_3C_2$ phase in the molten and resolidified nickel matrix resulted in a reduction in surface roughness. This is an advantage as it reduces the time and cost of surface treatment (grinding and polishing) (G.-S. Ham et al., 2021). As the spray distance increased, the roughness of the coatings increased. In addition, as the spray distance increased, the temperature of the particles in flight within the flame decreased, resulting in a higher number of cold particles outside the flame. As a result, a developed coating surface is formed, characterized by high roughness.

The factors influencing the hardness of thermally sprayed coatings are the features of the microstructure, phase composition and porosity content. The results show that the $Cr_3C_2$ -25NiCr coating sprayed at a distance of 200 mm HVOF demonstrates high microhardness (about 650 HV). Which is almost 2 times higher than the hardness of copper. High hardness is useful for wear resistance, as solid carbide can effectively compensate for external stress.

As the distance increased, the hardness of the coatings diminished ($L_1$=654±15HV $_{0.1}$; $L_2$=627.96 ±15HV $_{0.1}$; $L_3$=373.3±15HV $_{0.1}$). The volume fraction of carbides in the phase composition of the coating at a spray distance of 200 mm (Figure 2) proves that the hardness of the coating depends on the degree of decarburization, that is, the higher the degree of decarburization, the lower the hardness. This is due to the influence of higher kinetic energy of particles on the release of carbides sprayed at shorter distances and an increase in the number of dislocations (Hamatani, Ichiyama and Kobayashi, 2002; J. G. La Barbera-Sosa et al., 2010). A higher particle velocity can be achieved at a relatively higher pressure and a shorter spray distance. With increasing velocity, particles have higher kinetic energy. When the particles collide with the substrate, this kinetic energy is converted into thermal energy. Thus, for particles with a higher velocity, the amount of deposited carbide may increase and the hardness will increase. Another possible reason is related to the density of dislocations in the coating. At higher speeds, higher kinetic energy can lead to increased dislocation density and hardness.

As the spraying distance increases, the friction coefficient of the $Cr_3C_2$-NiCr coating also rises. Figure 6 illustrates the correlation between the friction coefficient and the sliding distance.

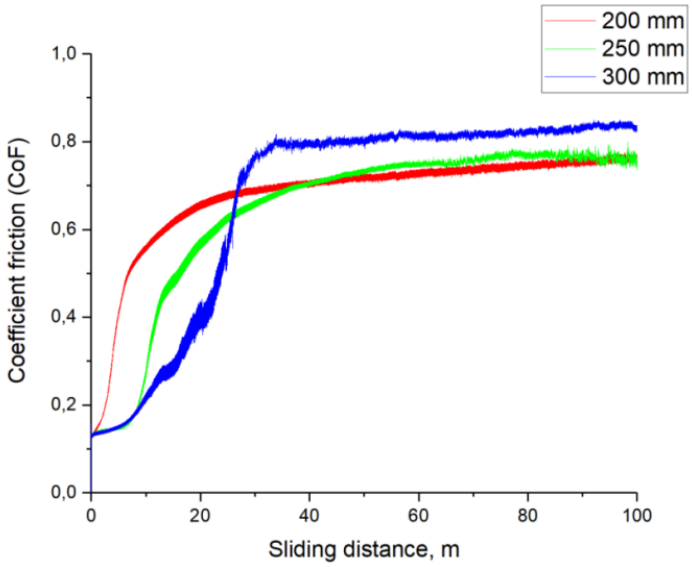


**Figure 6.** Graph of the dependence of the coefficient of friction on the sliding distance
*Note – compiled by the authors*

The friction coefficient of the coatings produced at different spraying distances is as follows: $L_1$ – 0.7; $L_2$ – 0.75; $L_3$ – 0.8. Samples $L_1$, $L_2$ showed a more stable CoF after the lapping stage, however, a slight fluctuation in the sample $L_2$ can be noticed after reaching a sliding distance of about 90 m. The sprayed $L_3$ coatings showed a higher CoF than the rest of the coatings. It should be noted that coatings with a lower coefficient of friction can help reduce the wear rate (Govande et al., 2022).

Conclusions. X-ray analysis of the initial $Cr_3C_2$-25NiCr powder and sprayed coatings by HVOF showed the presence of two main phases: binding $CrNi_3$ and solid $Cr_3C_2$. The phases $Cr_7C_3$ and $Cr_{23}C_6$ were found in the coatings, which indicates the decarburization process of $Cr_3C_2$. The analysis of the diffractogram revealed a detrimental effect of the $Cr_3C_2$ phase decomposition on the microhardness of the coating. A reduction in distance results in an increase in the intensity of the chromium carbide $Cr_3C_2$ peaks in the coatings. It was revealed that the NiCr binding phase was not detected in the $L_3$ coating, but $Cr_{23}C_6$ was formed instead due to decarbonization of the carbide phase. It was revealed that the main diffraction peaks of $Cr_7C_3$ and $Cr_{23}C_6$ may coincide with the lines related to NiCr and $Cr_3C_2$, which makes it difficult to uniquely identify them by X-ray diffraction. It has been established that the decarburization of $Cr_3C_2$ is associated with heating of spray particles, which can lead to carbon loss and a change in the content of carbides in coatings.

The morphology of the cross-section of coatings obtained at different deposition distances is characterized by a predominance of dark gray contrast particles, which presumably correspond to the $Cr_3C_2$ phase, and a lighter gray matrix, probably representing a matrix with a high nickel content. It was observed that the coating thickness reduced as the spraying distance increased. The coating thicknesses for $L_1$, $L_2$, and $L_3$ were 120.91 μm, 47.63 μm, and 16.6 μm, respectively. $L_1$ exhibited strong adhesion to the substrate. It has been established that plastic deformation of carbide particles is observed in coatings $L_2$ and $L_3$, which may indicate stress concentration in these samples.

It was observed that the average surface roughness of the coatings $L_1$, $L_2$ and $L_3$ is respectively $R_a$ = 0.672 microns, $R_a$ = 0.743 microns and $R_a$ = 0.808 microns, which indicates the dependence of this parameter on the spraying distance. It was noted that as the spraying distance increased, the roughness of the coatings also increased. This can be attributed to a higher number of cold particles outside the hot flame center, leading to the formation of a more developed coating surface. It was determined that the $Cr_3C_2$-25NiCr HVOF coating sprayed at a distance of 200 mm demonstrates a high microhardness of about 650 HV, which is almost 2 times higher than the hardness of copper, which is important for increasing the wear resistance of coatings. It has been established that increasing the spraying distance increases the friction coefficient of the $Cr_3C_2$-NiCr ceramic coating, which is confirmed by the values of the coefficient of friction for coatings $L_1$ (0,7), $L_2$ (0,75) and $L_3$ (0,8).

*Conflict of interest.* The author(s) declare that there is no conflict of interest.

*Acknowledgments.* This research has been funded by the Committee of Science of the Ministry of Science and Higher Education of the Republic of Kazakhstan (Grant No. BR24992864)

*Notice of the use of generative AI and AI-enabled technologies in the writing of the manuscrip.* The author group did not use generative AI in the preparation of this article.

References

Liu J., Zhu C., Li G. Application Research Progress of Coatings on Copper Plate in Continuous Casting Mould // Cailiao Daobao/Materials Reports. – 2019. – Vol. 33. – P. 2831-2838.

Moro L., Srnec Novak J., Benasciutti D., De Bona, F. Copper mold for continuous casting of steel: Modelling strategies to assess thermal distortion and durability. In Key Engineering Materials. – 2017. –Vol. 754. – P. 287-290.

Ryu M., Choi H., Yoon J., Choi Y. N., Lee S., Kim H. Lee H. Silica-nanoparticle reinforced lubricant-infused copper substrates with enhanced lubricant retention for maintenance-free heat exchangers. Chemical Engineering Journal, 2023. – Vol. 451. – P. 138657.

Moro L, Srnec Novak J, Benasciutti D, De Bona F. Thermal distortion in copper moulds for continuous casting of steel: numerical study on creep and plasticity effect. Ironmaking & Steelmaking. – 2019. – Vol. 46(1). – P. 97-103.

Velička M., Pyszko R., Příhoda M., Molínek J. Research of heat transport in mould for continuous casting of steel. Metalurgija. – 2009. – Vol. 48(4). – P 277-280.

Swain A. N. S. S., Choudhary S. K., Ganguly S., Rajasekar K., Golani R., Singh V. Effect of initial solidification characteristics on longitudinal crack formation in thin slab caster. Canadian Metallurgical Quarterly, 2023. – Vol. 62(2). – P 372-382.

Novak, J.S., Lanzutti, A., Benasciutti, D., De Bona, F., Moro, L., & De Luca, A. Metallurgical and surface damage analysis in a copper mold after service. In Materials Today: Proceedings. – 2018. – Vol. 5. – P 26709-26714.

Berger L. M. Application of hardmetals as thermal spray coatings // International Journal of Refractory Metals and Hard Materials. – 2015. – Vol. 1 (49). – P. 350-364.

Bolelli, G., Berger, L. M., Börner, T., Koivuluoto, H., Matikainen, V., Lusvarghi, L., Vuoristo, P. Sliding and abrasive wear behaviour of HVOF- and HVAF-sprayed $Cr_3C_2$-NiCr hardmetal coatings. Wear, -2016. Vol.32. – P. 358-359.

Akhtari Zavareh, M., Sarhan, A. A. D. M., Razak, B. B., & Basirun, W. J. The tribological and electrochemical behavior of HVOF-sprayed $Cr_3C_2$-NiCr ceramic coating on carbon steel. Ceramics International, -2015, - Vol. 41(4). – P. 5387-5396.

Guilemany, J.M., Nutting, J., Sobolev, V.V., Dong, Z., De Paco, J.M., Calero, J.A., & Fernandez, J. Interface structures of high velocity oxy-fuel sprayed WC-Co coating on a copper substrate. Materials Science and Engineering. – 1997. – Vol. 232(1-2). – P. 119-128.

Yang K., Chen C., Xu G.Z., Zhang S.H. Application Status and Prospects of Thermal Spraying Technology in Metallurgical Field under Harsh Service Environment. Surface Technology. – 2022. – Vol. 51(1). – P. 16-32.

Zhu C., Wang W., Lu C. Characterization of cermet coatings and its effect on the responding heat transfer performance in strip casting process // Journal of Alloys and Compounds. – 2019. – Vol. 770. – P. 631-639.

Govande, A. R., Chandak, A., Sunil, B. R., & Dumpala, R. Carbide-based thermal spray coatings: A review on performance characteristics and post-treatment. International Journal of Refractory Metals and Hard Materials. Elsevier Ltd. – 2022, February 1. – Vol.103. – P. 105772.

Zhang, Y., Chong, K., Liu, Q., Bai, Y., Zhang, Z., Wu, D., & Zou, Y. (2021). High-temperature tribological

behavior of thermally-treated supersonic plasma sprayed $Cr_3C_2$-NiCr coatings. International Journal of Refractory Metals and Hard Materials. – 2021. – Vol. 95. – P. 105456.

Alroy R. J., Kamaraj M., Sivakumar G. Influence of processing condition and post-spray heat treatment on the tribological performance of high velocity air-fuel sprayed $Cr_3C_2$-25NiCr coatings // Surface and Coatings Technology. – 2023. – Vol. 463. – P. 129498.

Du J. Yu, Li F. Yi, Li Y. Le, Wang L. Ming, Lu H. Yang, Ran X. Ju, Zhang X. Yi. Influences of plasma arc remelting on microstructure and service performance of $Cr_3C_2$-NiCr/NiCrAl composite coating. Surface and Coatings Technology. – 2019. – Vol.369. – P.16-30.

Ham, G. S., Kreethi, R., Kim, H. jun, Yoon, S. hoon, & Lee, K. A. Effects of different HVOF thermal sprayed cermet coatings on tensile and fatigue properties of AISI 1045 steel. Journal of Materials Research and Technology. – 2021. – Vol.15. – P. 6647-6658.

Zimmermann S., Kreye H. Chromium Carbide Coatings Produced with Various HVOF Spray Systems. Proceedings from the National Thermal Spray Conference.International Thermal Spray Conference. – 1996. – P. 147-152.

Mahade, S., Mulone, A., Björklund, S., Klement, U., & Joshi,S. Investigating load-dependent wear behavior and degradation mechanisms in $Cr_3C_2$–NiCr coatings deposited by HVAF and HVOF. Journal of Materials Research and Technology. – 2021. – Vol. 15. – P. 4595-4609.

Matikainen V., Koivuluoto H., Vuoristo P. A study of $Cr_3C_2$-based HVOF- and HVAF-sprayed coatings: Abrasion, dry particle erosion and cavitation erosion resistance // Wear. – 2020. – Vol. 446-447. – P. 203188.

Ozkan D. Structural characteristics and wear, oxidation, hot corrosion behaviors of HVOF sprayed $Cr_3C_2$-NiCr hardmetal coatings // Surface and Coatings Technology. – 2023. – Vol. 457. – P. 129319.

Shi, C., Liu, S., Irfan, Gong, Q., Wang, H., & Hu, M. Deposition mechanisms and characteristics of nano-modified multimodal $Cr_3C_2$-NiCr coatings sprayed by HVOF. Reviews on Advanced Materials Science. – 2022. – Vol.61(1). – P. 526-538.

Maheshwaran, S., Muthukumar, J., Gobalakrishnan, B., & Thirumani, K. S. (2022). Influence of $Cr_3C_2$ / NiCr Coating on Stainless Steel and Optimization of Mechanical Properties by Thermal Sprayed High Velocity Oxy-Fuel Coatings. – 2022. – Vol. 4(3). – P. 1-14.

Tillmann, W., Kuhnt, S., Baumann, I.T. et al. Statistical Comparison of Processing Different Powder Feedstock in an HVOF Thermal Spray Process. J Therm Spray Tech.- 2022. Vol. 31. – P. 1476-1489.

He J., Lavernia E. J. Precipitation phenomenon in nanostructured $Cr_3C_2$–NiCr coatings // Materials Science and Engineering: A. – 2001. – Vol. 1 (301). – P. 69-79.

Muthu S. M., Arivarasu M., Krishna T. H., Ganguly S., Prabhakar K. V. P., Mohanty, S. Improvement in hot corrosion resistance of dissimilar alloy 825 and AISI 321 $CO_2$-laser weldment by HVOF coating in aggressive salt environment at 900°C. International Journal of Minerals, Metallurgy and Materials, 2020. – Vol.27(11). – P. 1536-1550.

Sahraoui T., Fenineche N. E., Montavon G., Coddet C. Structure and wear behaviour of HVOF sprayed $Cr_3C_2$-NiCr and WC-Co coatings. Materials and Design. – 2003. – Vol. 24(5). – P. 309-313.

Wang R., Ye S., Xie Z., Zhang Z., Han H., Hong J., Lu X. Effect of copper oxides on defect formation during PTA cladding of Stellite 6 on copper substrates. Surface and Coatings Technology. – 2023. – Vol. 466. – P. 129625.

Information about authors

**Abizhanova Indira –** Doctoral student, D. Serikbayev East Kazakhstan technical university, Ust-Kamenogorsk, Kazakhstan, E-mail: www.indiko@mail.ru, ORCID: 0009-0006-3218-7246, +7 771 179 79 37.

**Buitkenov Dastan –** assoc.professor, PhD, **S**. Amanzholova East Kazakhstan university, Ust-Kamenogorsk, Kazakhstan, E-mail: Buitkenovd@mail.ru, ORCID: 0000-0002-0239-5849, +7 776 439 99 94

**Magazov Nurtoleu** – Doctoral student, D. Serikbayev East Kazakhstan technical university, Ust-Kamenogorsk, Kazakhstan, E-mail: magazovn@gmail.com, ORCID: 0000-0002-9941-9199, +7 747 426 30 19

**Kusainov Arystanbek** – Doctoral student, D. Serikbayev East Kazakhstan technical university, Ust-Kamenogorsk, Kazakhstan, E-mail: arys20055@gmail.com, Scopus Id: 59065558000, +7 707 783 70 60

**Abdulina Saule** – professor, PhD, D. Serikbayev East Kazakhstan technical university, Ust-Kamenogorsk, Kazakhstan, E-mail: abdulina.saule@mail.ru, +7 705 416 80 60